Łukasz J. NIEWIARA[1], Tomasz TARCZEWSKI[1], Lech M. GRZESIAK[2]

Nicolaus Copernicus University, Faculty of Physics, Astronomy and Informatics, Institute of Physics (1)
Warsaw University of Technology, Institute of Control and Industrial Electronics (2)

DC-DC converter based on silicon carbide (SiC) power devices with P+ based current controller

Abstract: *In this paper an investigation of voltage control system with P+ current controller for a DC-DC converter is presented. A DC-DC converter based on silicon carbide power devices were used. Synchronous buck topology is used for converter structure. Mathematical model of the converter is presented. The dependence between converter working conditions (i.e. input voltage, load current, switching frequency) and passive LC components is also given. A modified current control method based on P+ structure is considered. Proposed algorithm is compared with a traditional cascade structure based on PI type controllers. Output voltage and coil current dynamics were investigated. Experimental tests results were presented.*

Streszczenie: *W artykule przedstawiono wyniki badań układu regulacji napięcia przetwornicy DC-DC z regulatorem prądu typu P+. Zastosowano przetwornicę DC-DC z łącznikami na bazie węglika krzemu. Przetwornica została wykonana w topologii obniżającej napięcie. Przedstawiony został model matematyczny przetwornicy. Opisano także zależność pomiędzy warunkami pracy przetwornicy (np. napięcie wejściowe, prąd obciążenia, częstotliwość kluczowania) a parametrami elementów pasywnych LC. Przedstawiono propozycję struktury zmodyfikowanego regulatora prądu typu P+. Rozważany algorytm porównano z tradycyjnym algorytmem PI. Przedstawione badanie eksperymentalne dotyczą dynamiki napięcia wyjściowego oraz prądu dławika. (Przetwornica DC-DC na bazie węglika krzemu z regulatorem prądu typu P+).*

Keywords: DC-DC converter, buck topology, SiC MOSFET transistors, cascade control, voltage and current control.
Słowa kluczowe: przetwornica DC-DC, tranzystory SiC MOSFET, regulacja kaskadowa, regulacja napięcia i prądu.

Introduction

DC-DC converters are widely used in the process of electrical energy conversion. The use of switching DC-DC converters enables voltage and current conversion in an easy way. The growth of power electronics applications has increased the use of synchronous buck converters. This converter topology is one of the most common and is often used [1]. It became popular because of their compact size, simple structure and high efficiency [2]. Synchronous buck converter is usually used in high efficiency power supplies. Its high efficiency causes that, they are used instead of linear voltage regulators in high power solutions. In battery-powered applications, synchronous buck converters are most widely used. For example for control of charging current in advanced battery systems [2, 3]. In some applications they are used for direct control of DC motors instead of a traditional H-bridge based power circuit [4]. This solution allows to reduce motor current ripples and may improve control quality [4, 5]. One of a new field of buck converter application is a Voltage Matching Circuit in advanced inverter topologies [6].

In the last few years a significant increase of silicon carbide (SiC) power semiconductor popularity can be observed [7]. SiC based power devices have a lot of advantages in comparison to traditional Si elements. For example low on resistance (low conduction losses), very low switching losses, short rise and fall time (enables increase of switching frequency) and small total capacitance [8,9]. The use of SiC transistors and shottky diodes makes it possible to reach high efficiency (over 95%) for power converters and inverters [10,11]. The higher switching frequency gives a possibility to reduce the size of passive components. It results in device size reduction [11].

Control algorithms are essential issue in the regulation process. Because of easy implementation and well known tuning methods, Cascade Control Structure (CCS) with PID type controllers is the most popular structure [12]. An alternative to this method may be: state feedback control (LQR) [13, 14, 15], or fuzzy control [16, 17]. In this paper a modified CCS control structure with P+ current controller is presented. Dynamics of the control system with proposed P+ controller was compared with control system that includes traditional PI based CCS. System dynamics (i.e. output voltage, coil current response) was compared to traditional PI based CCS.
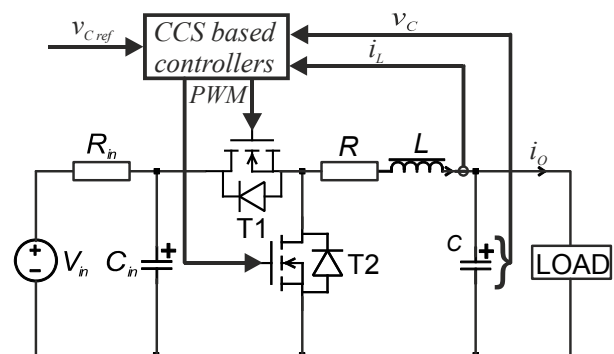
Fig.1. Proposed control system structure

DC-DC Converter topology

Non-isolated converter topology shown in Fig. 1 was investigated. In this solution a two way flow of energy (i.e. charging and discharging of output capacitor) can be realized. A LC filter is used to realize electrical output circuit of the converter. During switching of transistor T1 current flows through the coil and charges the output capacitor. This operation mode provides energy to the output. Switching of transistor T2 causes current flow from the output capacitor through the coil to the input circuit.

Mathematical model of considered buck converter with an output LC filter takes the following form [12]:

$$(1) \qquad V_{in}(t) = R\, i_L(t) + L\frac{d\, i_L(t)}{dt} + v_C(t)$$

$$(2) \qquad C\frac{dv_C(t)}{dt} = i_C(t)$$

$$(3) \qquad i_L(t) = i_C(t) + i_O(t)$$

where: $V_{in}(t)$ – input voltage, $i_L(t)$ – coil current, L, R - coil inductance and resistance, $v_c(t)$ – output voltage, C – *output capacitance*, $i_C(t)$ – capacitor current, $i_O(t)$ – load current.

In order to realize output voltage regulation Pulse Width Modulation method (PWM) was used. Transistors T1 and T2 are switched using a rectangular signal with constant period and variable duty factor. Parameters of the converter can be calculated by using the following equations [11]:

$$(4) \qquad L = \frac{V_{in}}{4 f_p \Delta i}$$

$$(5) \qquad C = \frac{i_O}{4 f_p \Delta v_C}$$

where: L, C – calculated value of inductance and capacitor capacitance, f_p – switching frequency, Δi – accepted coil current ripple value, Δv_c – accepted output voltage ripple value, i_O – average value of load current. Since switching frequency is parameter of denominator in (4) and (5), by using SiC power devices with higher f_p, smaller size passive elements for the same current and voltage ripple can be applied in comparison to Si based power devices.

Traditional PI based current control structure

In order to design current controller, equations (1) - (3) should be rewritten in a Laplace domain:

$$(6) \qquad \frac{I_L(s)}{V_{in}(s) - V_C(s)} = \frac{R^{-1}}{sT_e + 1}$$

$$(7) \qquad \frac{V_C(s)}{I_C(s)} = \frac{1}{sC}$$

$$(8) \qquad I_C(s) = I_L(s) - I_O(s)$$

where: T_e – electrical time constant ($T_e = L/R$). In order to obtain a simplified converter model it was necessary to introduce average input voltage signal instead of V_{in}. The dynamics of the power stage was approximated using proportional element K_{pp}. These operations allowed to obtain following equations:

$$(9) \qquad K_{pp} = V_{in}$$

$$(10) \qquad V_{in\,av}(s) = K_{pp}\delta(s)$$

where: K_{pp} – power stage input gain, $V_{in\,av}(s)$- average input voltage, $\delta(s)$ – PWM input signal duty value. Duty value is in range of {-1,1}. Negative value of duty means that transistor T2 is switched on. After putting (10) into (6), the following formula was obtained:

$$(11) \qquad \frac{I_L(s)}{\delta(s) - V_{Cn}(s)} = \frac{K_{pp}R^{-1}}{sT_e + 1}$$

where: $V_{Cn}(s)$- normalized output voltage ($V_{Cn}(s)=V_C(s)/K_{pp}$). The equation (11) represents the open-loop transfer function of the current path.
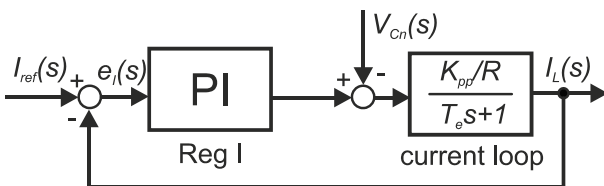
Fig.2. Current control loop with PI controller

In order to realize current control (Fig. 2) a PI controller was chosen. The transfer function of the regulator model is described by a following formula:

$$(12) \qquad G_R(s) = K_{pi}(\frac{1}{sT_{ii}} + 1)$$

where: K_{pi} – proportional gain, T_{ii} – integration time constant. Due to control signal limitations it was necessary to introduce an additional signal u_{awi} to avoid wind-up phenomenon. This signal is added to the integrator input.

$$(13) \qquad u_{awi}(s) = K_{awi}[u^*_{cc}(s) - u_{cc}(s)]$$

where: K_{awi} – control signal saturation error gain, $u^*_{cc}(s)$ – not saturated control signal, $u_{cc}(s)$– saturated control signal.

The use of microcontroller based control system causes that it was necessary to use discrete form of the control law. For that reason backwards Euler discretization method was applied to calculate discrete form of (12).

The result of mentioned operations is a discrete controller (Fig. 3) described by following equations:

$$(14) \qquad G_R(z) = K_{pi}(\frac{T_s z}{T_{ii}(z-1)} + 1) + u^*_{awi}(z)$$

$$(15) \quad u^*_{awi}(z) = \frac{T_s z}{T_{ii}(z-1)} K_{awi}[u^*_{cc}(z) - u_{cc}(z)]$$

where: T_s – sample time, $u^*_{awi}(z)$ – integrated anti-wind up signal.
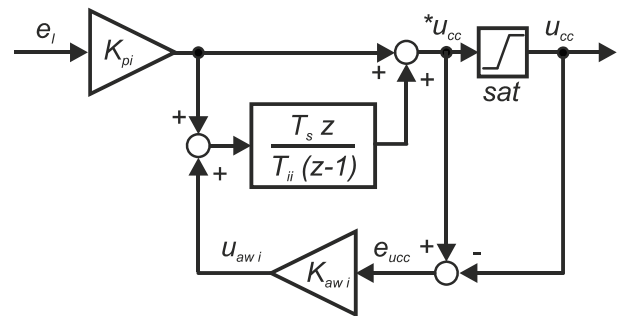
Fig.3. Discrete PI current controller structure

Proposed current control structure

It is well known, that using of integration path in control algorithm may causes a deterioration of system dynamics. It is necessary to use additional anti wind-up structure for proper operation of the PI type controller. On the other hand, it is well known, that the absence of integral operation causes a steady-state error in most cases. In order to achieve better dynamics properties of current control loop and zero steady-state error the modified control structure was proposed. It is based on proportional path only and it is named P+. Transfer function of closed loop current path with proportional element can be approximated by:

$$(15) \qquad G_C(s) \cong \frac{1}{s\dfrac{L}{K_{pi}K_{pp}} + 1}$$

The dynamics of the response can be affected by setting the proportional element gain - K_{pi}. The elimination of steady state error needs to consider the mathematical

model at steady state. Thus, (1) must be transformed taking into account (9) and (10), as follows:

$$(16) \qquad \delta_{steady}(t) = \frac{R}{K_{pp}} i_{ref}(t) + \frac{1}{K_{pp}} v_C(t)$$

where: δ_{steady} – steady state control signal duty value. It should be mentioned that in steady state the coil current is constant and equal to the reference value, so the di_L/dt is equal zero.
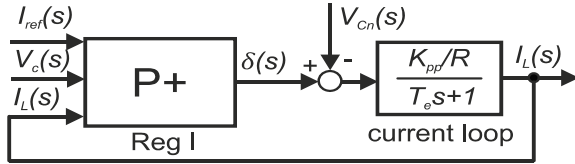
Fig. 4. Current control loop with P+ controller

In this case the control law of P+ algorithm is a combination of proportional control and steady state input (δ_{steady}):

$$(17) \qquad \delta(t) = K_{pi} e_i(t) + K_i\, i_{ref}(t) + K_v v_C(t)$$

where: K_i – reference current gain ($K_i=R/K_{pp}$), K_v – output voltage gain ($K_v=1/K_{pp}$).
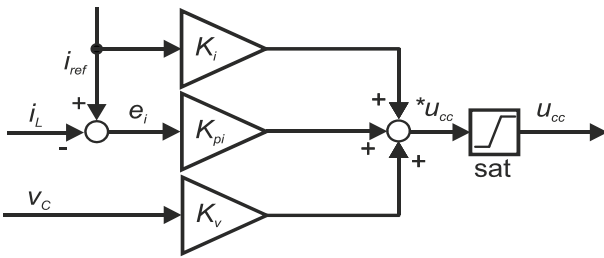
Fig.5. P+ current controller structure

The considerations presented above are valid only for $\delta \geq 0$ otherwise (15) and (16) should be modified. When the duty signal is smaller than zero it means that the transistor T2 will be switched on. The energy is received from the capacitor, so the output capacitor voltage becomes the input voltage source. In this case the mathematical model of the system changes as follows:

$$(18) \qquad \delta(t) v_C(t) = R i_L(t) + L \frac{d i_L(t)}{dt}$$

The transfer function takes the form:

$$(19) \qquad \frac{I_L(s)}{\delta(t)} = \frac{V_C(s)}{T_e s + 1}$$

It can be seen that the gain of the model is depend on the output voltage. In such a case, model is non-linear and the transfer function of model also. In this case the transfer function of closed loop current path with proportional element can be approximated by:

$$(20) \qquad G_C'(s) \cong \frac{1}{\dfrac{L}{K_{pi}' V_C(s)} s + 1}$$

where: K_{pi}' – proportional gain for nonlinear operation mode. To obtain similar dynamics for both working conditions (i.e. charging and recharging mode), the time constants of $G_C(s)$ and $G_C'(s)$ should be equal. This dependence allows to determine K_{pi}', as follows:

$$(20) \qquad K_{pi}'(s) \cong K_{pi} \frac{K_{pp}}{V_C(s)}$$

It can be seen that during output capacitor discharging the proportional element gain depends on the output voltage. The gain should be calculate in each control loop. For steady state equation (18) should be taken in the account. The coil current is constant and equal to its reference value, so the di_L/dt is equal zero. In respect of this it is possible to obtain the following dependence:

$$(21) \qquad \delta_{steady}'(t) = \frac{R}{v_C(t)} i_{ref}(t)$$

The reference current gain is also dependent on the output voltage, so it should be calculated in each control loop too. For this case the control law of P+ controller is as follows:

$$(22) \qquad \delta'(t) = K_{pi}' e_i(t) + K_i'\, i_{ref}(t) + K_v' v_C(t)$$

where: K_i' – reference current gain ($K_i'=R/v_C(t)$), K_v' – output voltage gain ($K_v'=0$).

The values of P+ current controller gains are dependent on energy flow in the converter (Fig. 6). During energy providing mode ($i_L>0$) (17) control law should be used. It means that if the reference current is greater than or equal to zero, the controller gains are constant and equal to (17). For the other case ($i_L<0$) (22) control law should be used. In this operation mode the controller gains are not constant and dependent on the value of converter output voltage.
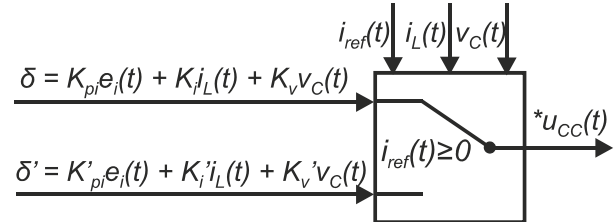
Fig.6. P+ controller mode selection

Voltage regulation

In order to realize voltage control a PI type controller (Fig. 7) was used. Controller transfer function is given as:

$$(23) \qquad G_{Rv}(s) = K_{pu}\left(\frac{1}{s T_{iu}} + 1\right)$$

where: K_{pu} – proportional element gain, T_{iu} – integrator time constant.
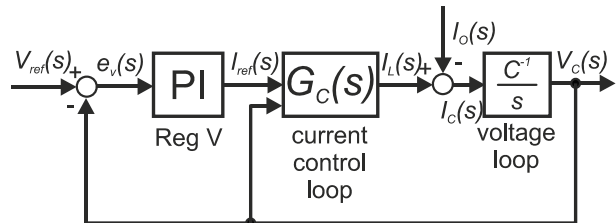
Fig.7. Voltage control loop

Due to coil current limitations it was necessary to introduce an additional signal u_{awu} to avoid wind-up

phenomenon. This signal is added to the integrator input to modify its output during controller output signal saturation.

$$(24) \qquad u_{awu}(s) = K_{awu}[I^*_{ref}(s) - I_{ref}(s)]$$

where: K_{awu} – reference current signal saturation error gain, $I^*_{ref}(s)$ – not saturated current reference signal, $I_{ref}(s)$– saturated control signal, should not exceed nominal current value I_n.
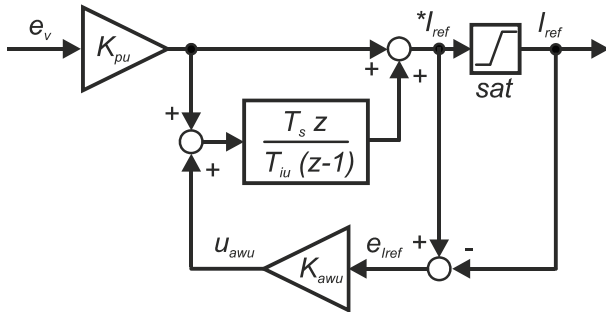
Fig.8. Discrete PI voltage controller structure

The use of microcontroller based control system causes that it was necessary to use discrete form of the control law in the regulation algorithm. For that reason it was required to discretize the continuous model (23). Backwards Euler discretization method was used. The result of mentioned operations is a discrete controller (Fig. 8) described by following equations:

$$(25) \qquad G_{Rv}(z) = K_{pu}\left(\frac{T_s z}{T_{iu}(z-1)} + 1\right) + u^*_{awu}(z)$$

$$(26) \quad u^*_{awu}(z) = \frac{T_s z}{T_{ii}(z-1)} K_{awu}[I^*_{ref}(z) - I_{ref}(z)]$$

where: T_s – sample time, $u^*_{awu}(z)$ – integrated anti-wind up signal.

Laboratory stand with DC-DC converter

The proposed control algorithm was tested on laboaratory stand with DC-DC converter. Silicon Carbide (SiC) based power MOSFET transistors (C2M0080120D) [19] and shottky diodes (C4D10120A) [20] were used as power devices. In order to realize coil current and capacitor voltage measurements LEM sensors were used, i.e. LTS15-NP for current sensing and LV-25P for voltage sensing. Electrical circuit parameters of the converter are summarized in Table 1.

Table 1. DC-DC converter parameters

Param.	Value	Unit	Param.	Value	Unit
V_{in}	120	[V]	R	0.3	[Ω]
C_{in}	470	[μF]	L	3.0	[mH]
I_N	3.0	[A]	C	30	[μF]
f_s	36	[kHz]	T_s	27.(7)	[μs]

Investigated control structures were implemented in dSpace DS 1104 R&D controller board. The maximum possible switching frequency was 36 kHz. Power resistors connected in parallel were used as load circuit. Load changes were realized using electrically controlled relays.
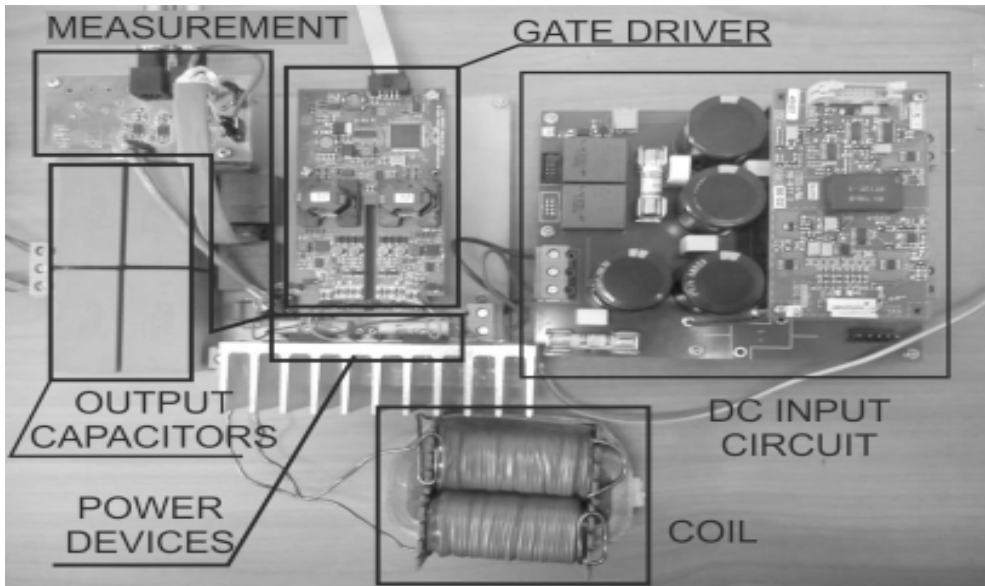
Fig.9. DC-DC converter

Experimental test results

The converter voltages and currents were measured by using TEKTRONIX TPS 2024B oscilloscope equipped with two A622 AC/DC current probes and two Tektronix P5122 voltage probes.

The controller settings were chosen empirically. As the current controller start point settings a modular optimum criterion was applied. As the voltage controller start point settings a symmetric optimum criterion was used. Due to limitation of maximum current and control signal values, it was necessary to retune the controller. It was assumed that the current peak should not exceed 3.5 A and the nominal

current value in normal operation mode is 3 A. Table 2 contains controller settings obtained after tuning process for PI based CCS. It was a compromise between the dynamics and signal quality.

Table 2. PI type controllers settings

Voltage controller		Current controller	
K_{pu}	0.12	K_{pi}	0.3
T_{iu}	3.0e-3	T_{ii}	1.0e-3
K_{awu}	-6.0	K_{awi}	-4.0

The voltage controller settings for CCS with P+ current controller were also chosen empirically. The start point was

chosen using symmetric optimum criterion. Table 3 contains controller settings obtained after tuning process. The proportional gain K_{pi} in current controller structure was chosen to obtain the best possible dynamic of output voltage response considering current and control signal limitations. The dynamics of the current loop is determined by the proportional gain. Increase of the gain value improves the dynamics but it also may cause some overshoot.

Table 3. CCS with P+ controller settings

Voltage controller		Current controller	
K_{pu}	0.2	K_{pi}	0.35
T_{iu}	2.0e-3	K_i	2.5e-3
K_{awu}	-6.0	K_v	8.3e-3

The dynamics of current loop has a direct impact on the dynamics of voltage loop. The use of a P+ controller in current path allows to change the settings of voltage controller and in effect improves system dynamics.
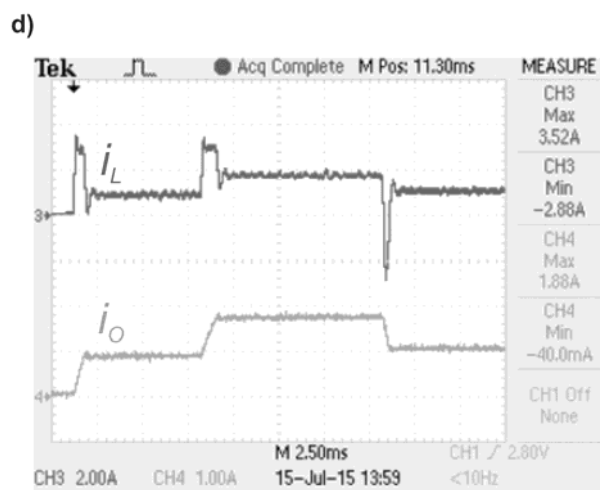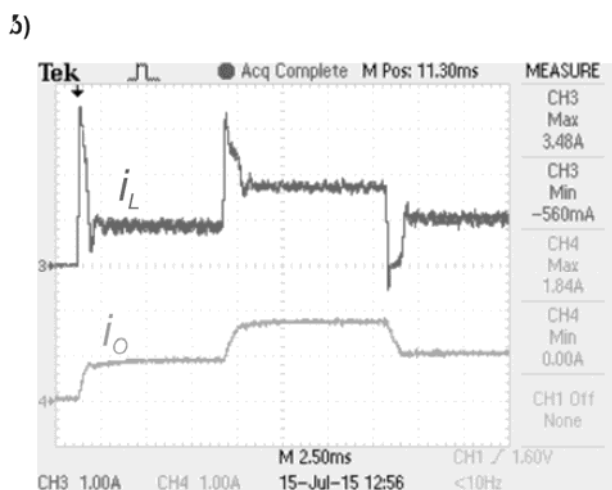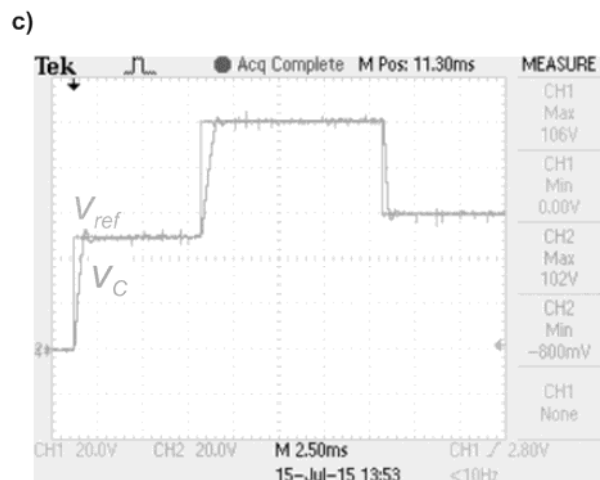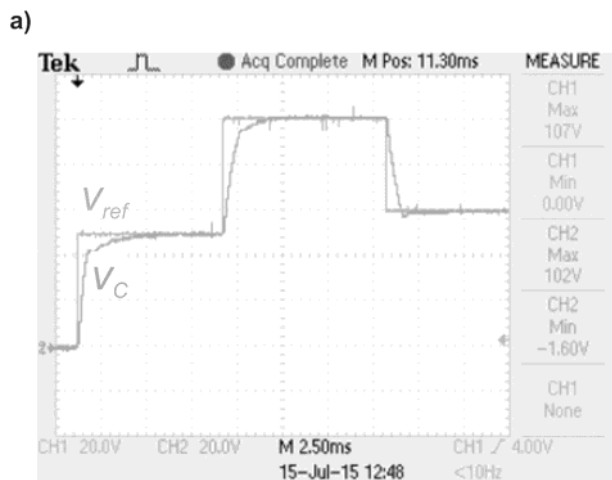
Fig.10. Output voltage and current waveforms: a) output voltage CCS with PI-PI, b) coil and load current waveforms for CCS with PI-PI, c) output voltage for CCS with PI-P+, d) coil and load current waveforms for CCS with PI-P+

The behavior of the DC-DC converter is shown in Fig. 10. The left column contains the voltage and currents waveforms for CCS with PI type controllers. The right column contains voltage and currents waveforms for CCS with P+ current controller. It can be seen that for reference voltage variations (at t = 0ms reference increases to 50V, at t = 8ms reference increases to 100V and at t = 17ms reference decreases to 60V) the coil current i_L doesn't exceed the limitations in both control structures (Fig. 10: b and d). Cascade Control Structure based on P+ current controller in comparison to PI based structure improves the output voltage dynamics (Fig. 10: a and c). In this case the rise and regulation times are much smaller for P+ based CCS. There is a very small overshoot, which doesn't exceed 2%. A better dynamics of coil current (Fig. 10: b and d) was also obtained. The P+ current controller significant improves the dynamics of coil current response.

It becomes more sharp in case of reference voltage changes and the current waveform is more rectangular.

A very important control system feature is the reaction for load changes (i.e. load current). Load variations cause output signal distortion. This effect is undesirable and a properly functioning control system should compensate it. For this reason some tests were carried out for constant reference value and variable load. The output voltage reference value was set to 40V. At time t = 0ms the steady state load current value was set to 0.67 A, at time t = 13ms the load increases to 2.0 A and at time t = 27ms the load decreases to 0.67 A. The output voltage and currents waveform is shown in Fig. 11. It can be seen that full PI based CCS behavior in variable load operation mode is worse in comparison to CCS with P+ current controller. The voltage spikes and the return time are smaller using control

structure with P+ controller. Thanks to use of modified CCS, the system is more rigid and reacts faster for load changes.

The P+ current controller improves the dynamics of coil current loop (Fig. 12). It should be noted that PI based current controller has a significantly longer regulation time (Fig.12:a). It is caused by the integration path that introduces additional dynamics into control system. The output voltage influences the current path as given in (6) and it may have a significant impact on coil current behavior. To avoid this effect, the integrator gain should be increased, but due to system limitations it's not possible for this case. The modified controller structure (i.e. P+) does not include integration action in its structure. Instead, it introduces an additional δ_{steady} signal. This solution improves the current loop dynamics (Fig. 12:b).

a)
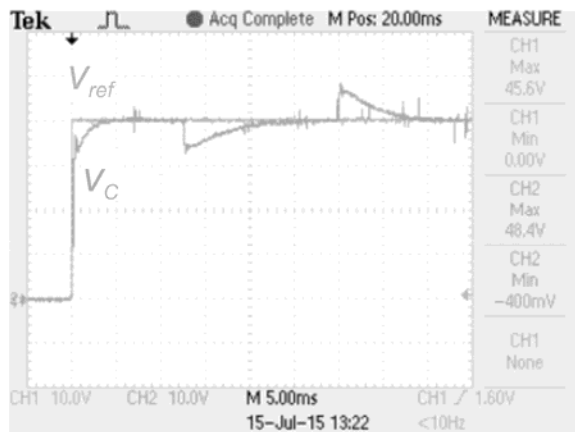
c)
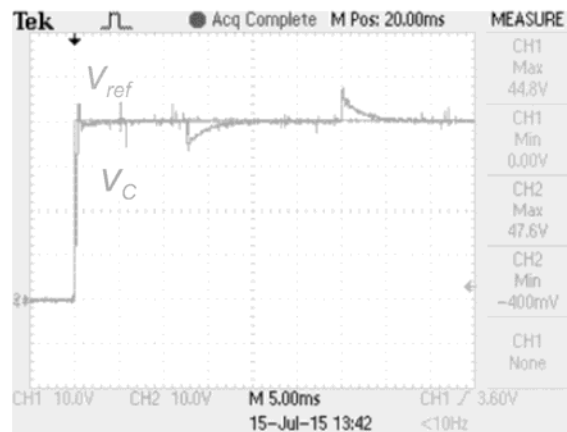
b)
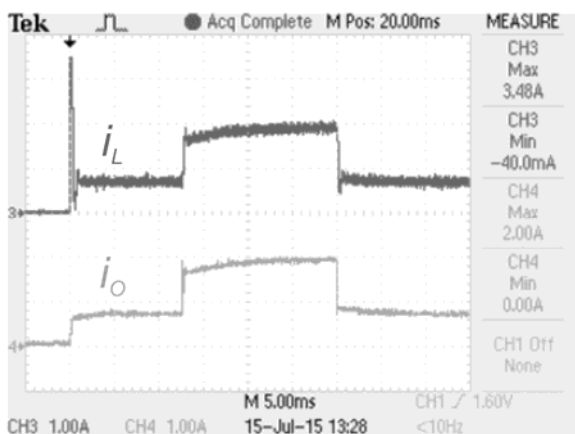
d)
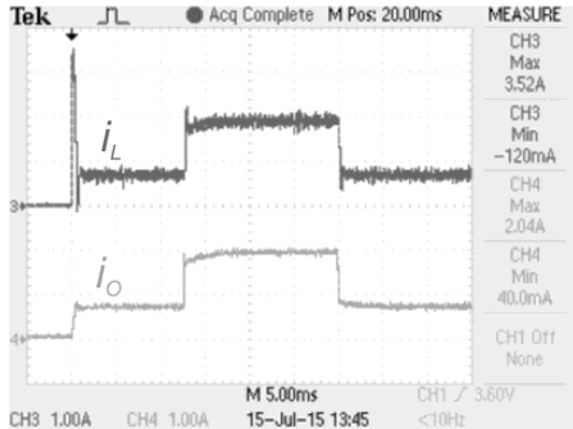
Fig.11. Output voltage and current waveforms during variable load operation: a) output voltage for CCS with PI-PI, b) coil and load current waveforms for CCS with PI-PI, c) output voltage for CCS with PI-P+, d) coil and load current waveforms for CCS with PI-P+

a)
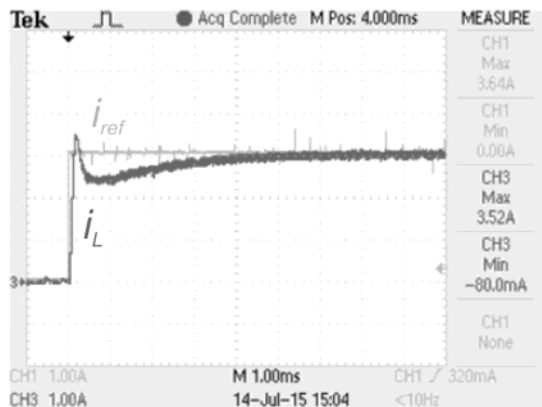
b)
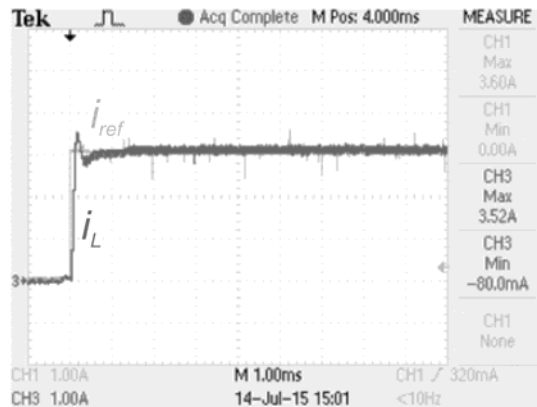
Fig.12. Coil current waveform in current control mode: a) coil current for PI based controller, b) current for P+ based controller

Conclusion

Cascade control structure based with P+ current controller improves the output voltage dynamics. The use of P+ current controller allows to set a bigger value of proportional gain for the voltage control loop. Thank this property, regulation and rise times are shorter than with full PI based structure. During load changes the control system reacts faster which results in voltage spikes reduction and faster load compensation.

P+ structure doesn't contain integral action. That allows to eliminate additional current controller dynamics (integration time). Current control based on such a solution reacts faster for output voltage changes, taking into account output voltage by control signal determining. For integration free controller, the use of anti-wind up loop in controller structure is not necessary. The dynamics of coil current loop can be set using only one proportional gain K_{pi}, other gains are determined by converter parameters (i.e. input voltage and coil resistance). The proposed controller structure significantly improves the dynamics of current loop response.

Authors:
mgr inż. Łukasz J. Niewiara, Nicolaus Copernicus University, Institute of Physics, Faculty of Physics, Astronomy and Informatics, Grudziądzka 5, 87-100 Toruń, E-mail: lukniewiara@fizyka.umk.pl
dr inż. Tomasz Tarczewski, Nicolaus Copernicus University, Institute of Physics, Faculty of Physics, Astronomy and Informatics, Grudziądzka 5, 87-100 Toruń, E-mail: ttarczewski@fizyka.umk.pl
prof. dr hab. Inż. Lech M. Grzesiak, Warsaw University of Technology, Institute of Control and Industrial Electronics, Koszykowa 75, 00-662 Warsaw, E-mail: l.grzesiak@isep.pw.edu.pl

REFERENCES
[1] Samosir A. S., Yatim A. H., Dynamic evolution control for synchronous buck DC-DC converter: Theory, model and simulation, *Simulation modeling Practice and Theory*, (2010), n.18, 663-676
[2] Gragger J. V., Haumer A., Einhorn M., Average model of a buck converter for efficiency analysis, *Engineering Letters*, (2010)
[3] Jiang Z., Dougal R. A., `1Synergetic control of power converters for pulse current charging of advanced batteries from a fuel cell power source, *IEEE Trans. on Power Electronics*, 19 (2014), n.4, 1140-1150`
[4] Linares-Flores J., Sira-Ramirez H., DC motor velocity control trough a DC-to-DC power converter, Proceedings of the IEEE conference on decision and control, 5 (2005), 5297-5302
[5] Linares-Flores J., Sira-Ramirez H., A smooth starter for a DC machine: a flatness based approach, International Conference on Electrical and Electronics Engineering and X Conference on Electrical Engineering, (2004), 589 – 594
[6] Tarczewski T., Niewiara L., Grzesiak L. M., Torque ripple minimization for PMSM using voltage matching circuit and neural network based adaptive state feedback control, IEEE *16th European Conference on Power Electronics and* Applications (EPE'14-ECCE Europe), 1-10
[7] Rabkowski J., Peftitsis D., Nee H. P., Silicon Carbide power transistors: a new era in power electronics is initiated, *IEEE Industrial Electronics Magazine*,`6 (2012), n.2, 17-26
[8] Shen M., Krishnamurthy S., Simplified loss analysis for high speed SiC MOSFET inverter, Twenty-Seventh Annual IEEE Applied Power Electronics Conference and Exposition (APEC), *(*2012), 1682-1687
[9] Zdanowski M., Rabkowski J., Barlik R., Comparative analysis of power losses in three phase PWM inverters with Silicon Carbide active devices (in Polish), *Przeglad Elektrotechniczny*, 87 (2011), n.10, 101-105
[10] Giziewski S., Three-phase voltage source inverter with SiC JFET transistors (in Polish), *Przeglad Elektrotechniczny*, 88 (2012) , n.4b, 76-79
[11] Niewiara Ł., Skiwski M., Tarczewski T., Grzesiak L. M., 9kW SiC MOSFET based DC-DC converter (IN PRESS)
[12] Raja Ismail R. M. T., Ahmad M. A., Ramli M. S., Speed control of buck-converter driven DC motor using LQR and PI: a `comparative assessment, International Conference on Information Management and Engineering, (2009), 651-655
[13] Moreira C. O., Silva F. A., Pinto S. F., Santos M. B., Digital LQR Control with Kalman estimator for DC-DC buck converter, IEEE EUROCON - International Conference on Computer as a Tool (EUROCON), (2011), 1-4.
[14] Dehghani H., Abedini A., Bina M. T., Advanced non-inverting step up/down converter with LQR control technique, Power Electronics, Systems & Technologies Conference, (2013), 254. 260
[15] Oliva A.R., Ang S. S., Bortoloto G. E., Digital control of a voltage-mode synchronous buck converter, *IEEE Trans. on Power Electronics*, 21 (2006), n.1, 157-163
[16] Wei, K. Sun Q., Liang B., Du M., The research of adaptive fuzzy PID control algorithm based on LQR approach in DC-DC converter, IEEE Pacific-Asia Workshop on Computational Intelligence and Industrial Application, (2008), 140-143
[17] Beid S. E., Doubabi S., Self-sheduled fuzzy control of PWM DC-DC Converters, Mediterranean Conference on Control & Automation, (2010), 916-921
[18] Niewiara Ł., Tarczewski T., Grzesiak L. M., 3-phase bridge voltage source inverter with DC voltage control (in Polish), *Przegląd Elektrotechniczny*, 90 (2014), n.6, 109-114
[19] CREE C2M0080120D data sheet available on the Internet at http: \\ www.cree.com\
[20] CREE C4D10120A data sheet available on the Internet at http:\\ www.cree.com\